

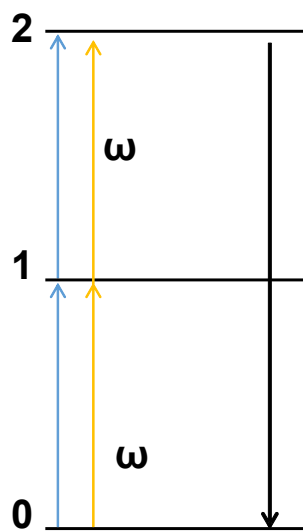
Supporting Information for

Record-High Hyperpolarizabilities in Atomically Precise Single Metal-Doped Silver Nanoclusters

*Hao Yuan, Isabelle Russier-Antoine, Christophe Moulin, Pierre-François Brevet, Željka
Sanader Maršić, Martina Perić Bakulić,* Xi Kang,* Rodolphe Antoine,* and Manzhou Zhu**

Table S1: Hyperpolarizability values for Au₂₅ and Ag₂₅ nanoclusters.^{1, 2} The plot of the HRS intensity for Au₂₅AcCys₁₈ nanoclusters as a function of concentration is given in Figure S12.

	Excitation wavelength (nm)	$\beta(2\omega)$ (10^{-30} esu)	references
Ag₂₅(DMBT)₁₈	950	516	This work
Au₂₅SG₁₈	802	128	Ref. 1
Au₂₅Cys₁₈	802	163	Ref. 1
Au₂₅AcCys₁₈	800	138	This work
Au₂₅p/m/oMBA₁₈	800	179, 203, 214	Ref. 2



Scheme S1: Resonant behavior of HRS if only two electronic excited state contributes.

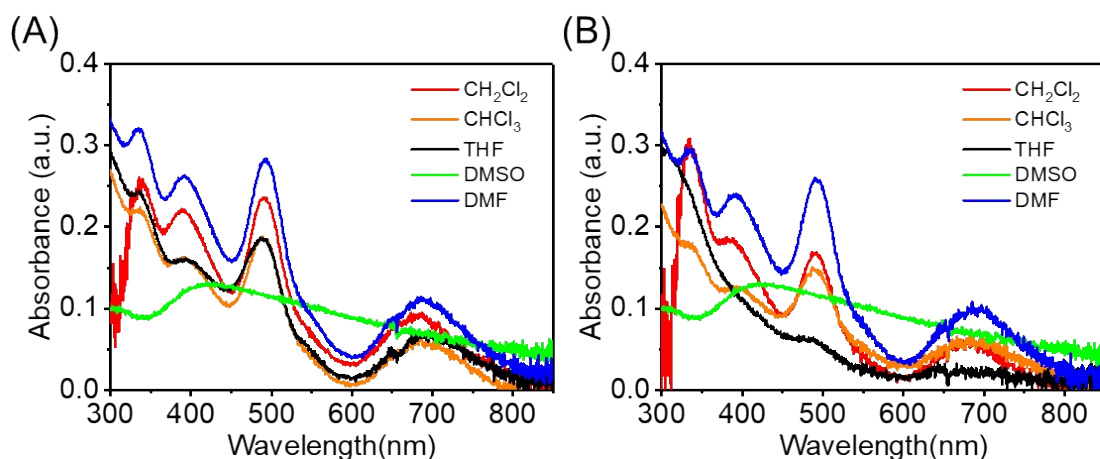


Figure S1. Absorption spectra of $\text{Ag}_{25}(\text{SR})_{18}$ in CH_2Cl_2 , CHCl_3 , THF, DMSO, DMF after fresh preparation (A) and after 1 day (B). $\text{Ag}_{25}(\text{SR})_{18}$ concentration: $2.74\mu\text{M}$. $\text{Ag}_{25}(\text{SR})_{18}$ in DMSO degraded within 10 mins; $\text{Ag}_{25}(\text{SR})_{18}$ in THF degraded after 1 day; $\text{Ag}_{25}(\text{SR})_{18}$ in CH_2Cl_2 , CHCl_3 , DMF can retain absorption feature after 1 day. (with SR=DMBT).

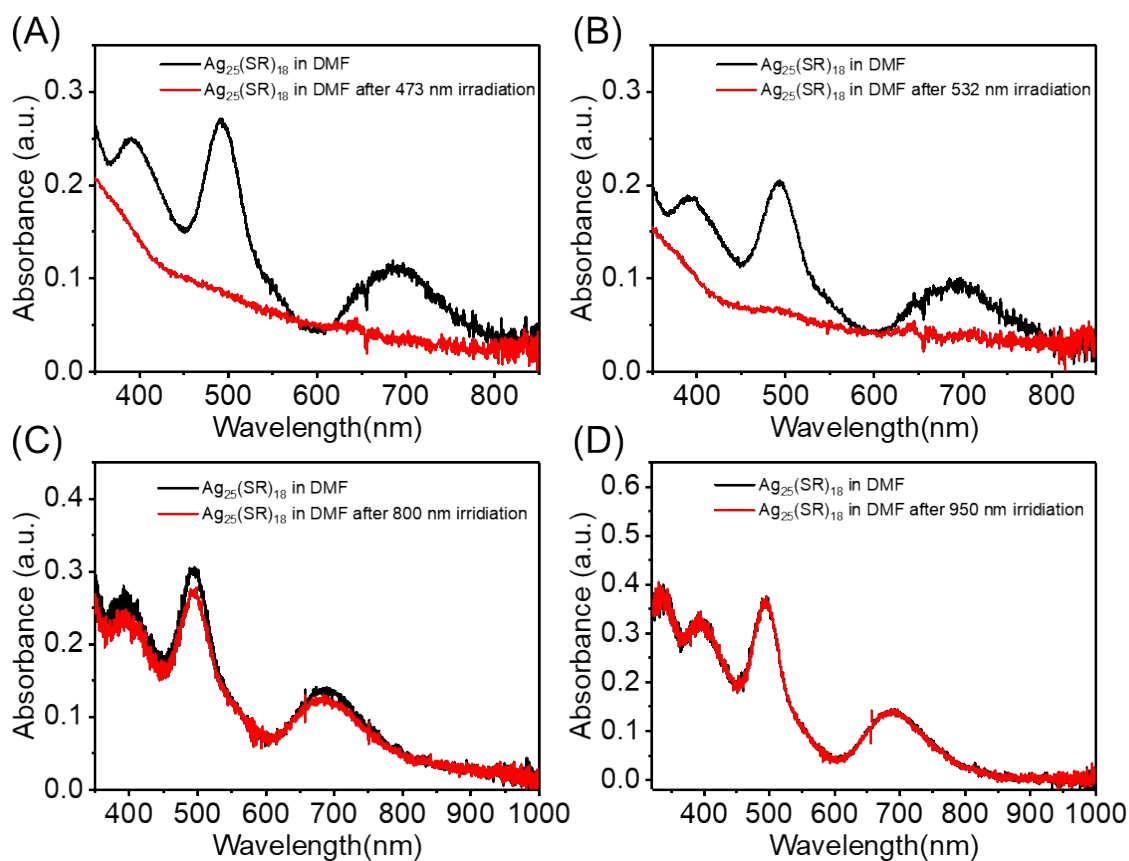


Figure S2: Absorption spectra of $\text{Ag}_{25}(\text{SR})_{18}$ before and after 2 mins laser irradiation. $\text{Ag}_{25}(\text{SR})_{18}$ was dissolved in DMF at $2.74\mu\text{M}$. (A) 473 nm continuous laser, 250 mW. (B) 532 nm continuous laser, 250 mW. (C) 800 nm femtosecond pulse laser, 400 mW. (D) 950 nm femtosecond pulse laser, 400 mW. (with SR=DMBT).

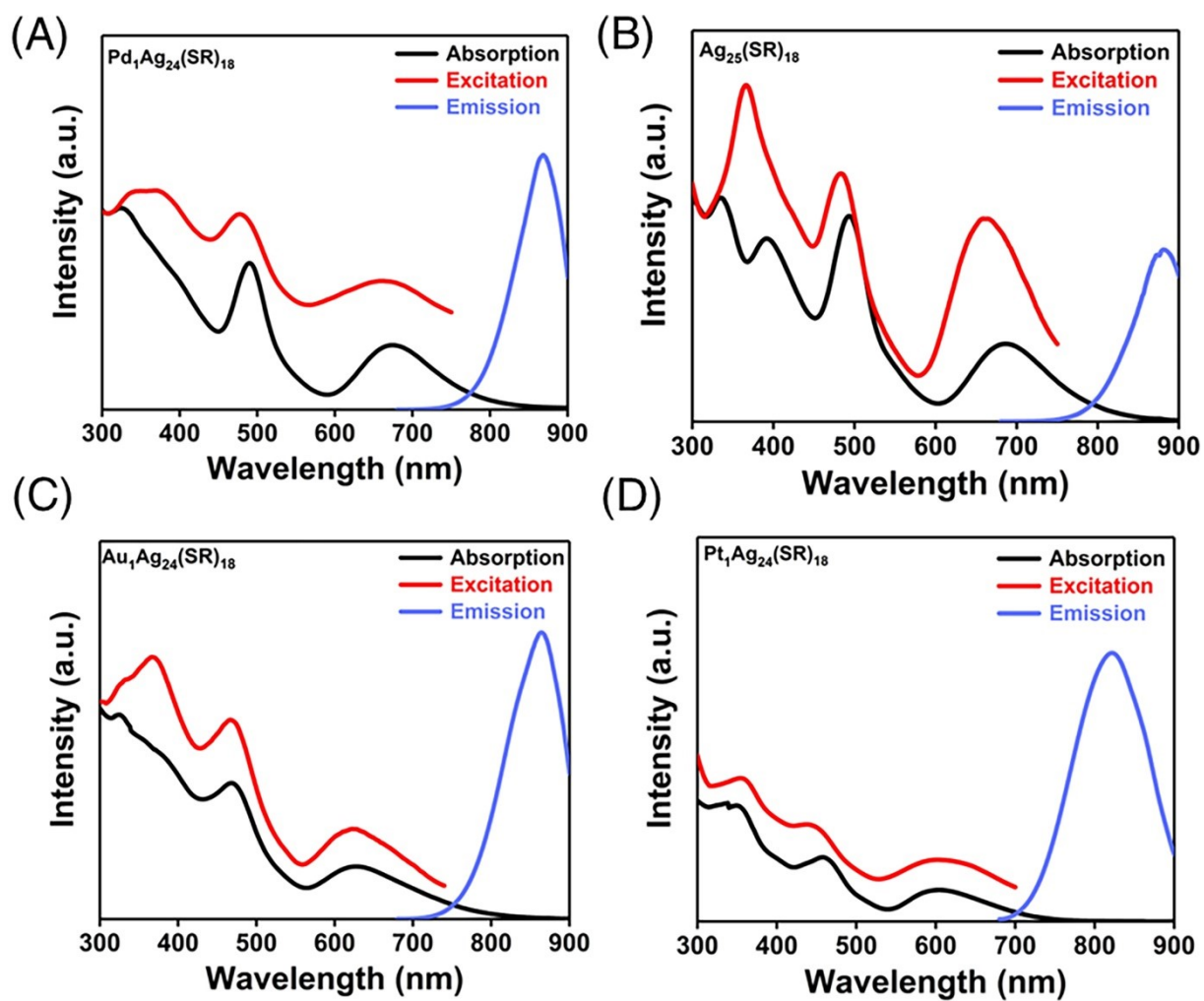


Figure S3: Absorption, excitation, and emission spectra of (A) $\text{Pd}_1\text{Ag}_{24}(\text{SR})_{18}$, (B) $\text{Ag}_{25}(\text{SR})_{18}$, (C) $\text{Au}_1\text{Ag}_{24}(\text{SR})_{18}$, and (D) $\text{Pt}_1\text{Ag}_{24}(\text{SR})_{18}$ nanoclusters in DMF. (with SR=DMBT)

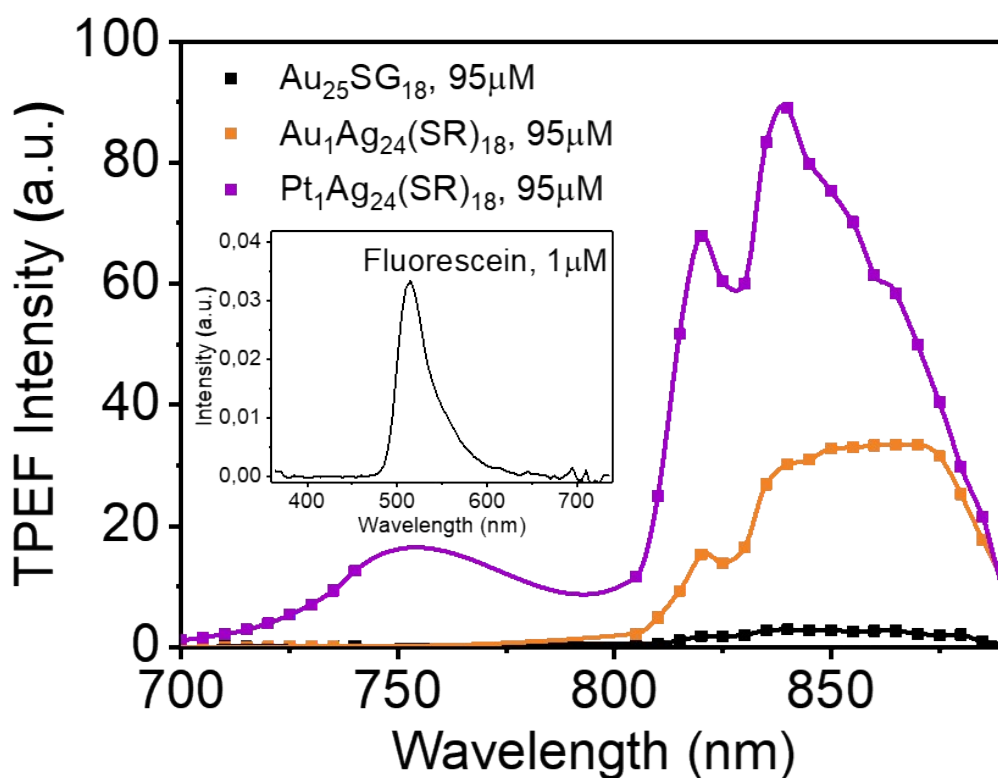


Figure S4. 2PEPL spectra with excitation at 780 nm of the synthesized Ag_{25} , $\text{Pt}_1\text{Ag}_{24}$, and $\text{Au}_1\text{Ag}_{24}$ nanoclusters dispersed in DMF. Inset 2PEPL spectrum of fluorescein for comparison. Of note, for $\text{Au}_{25}\text{SG}_{18}$ nanoclusters, a known 2PEPL cross section of $\sim 5 \text{ GM}$ was reported at 755 nm¹. (with SR=DMBT and SG=glutathione)

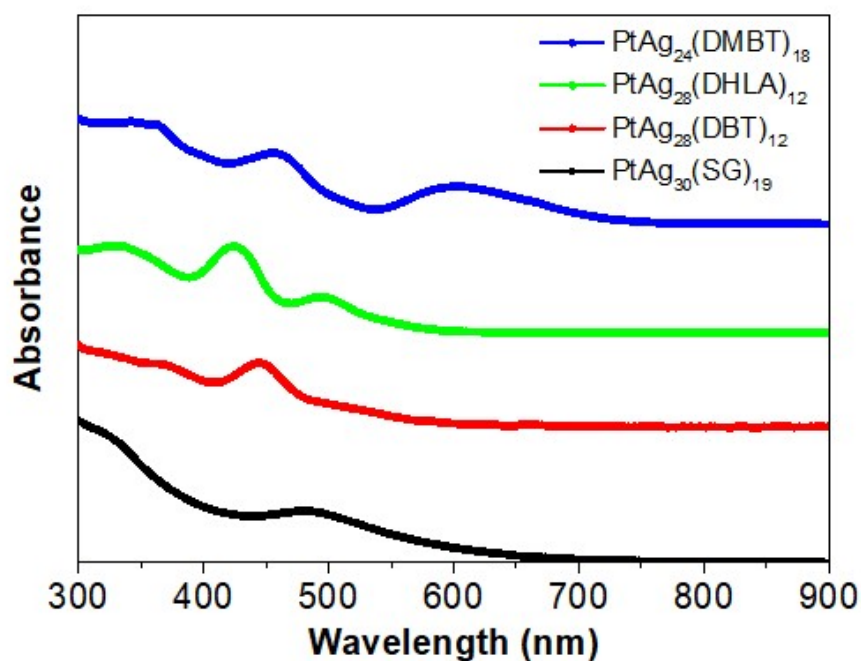


Figure S5. Absorption spectra of Pt doped silver nanoclusters. (cluster concentration 1mg/mL).

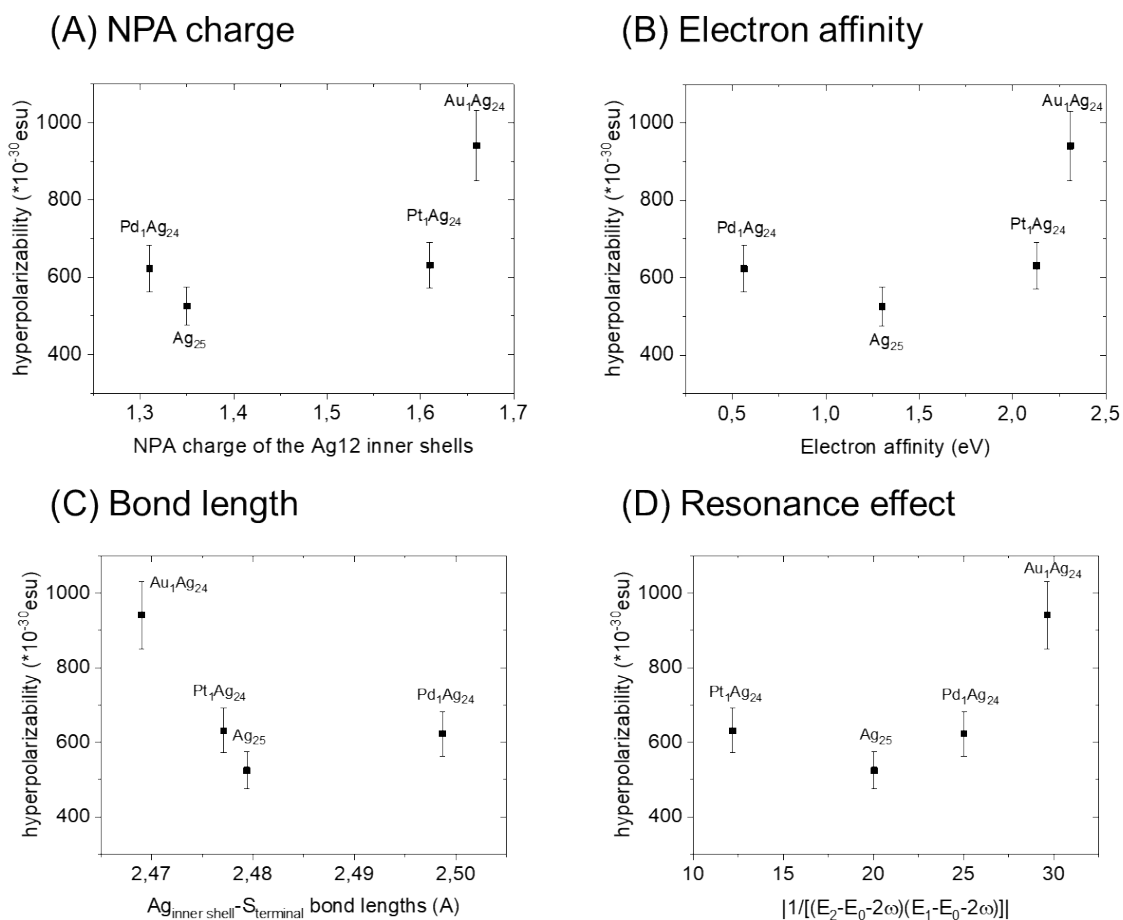


Figure S6. Plots of hyperpolarizability ($\beta(2\omega)$) values and some relevant properties of $M_1Ag_{24}(SR)_{18}$ nanoclusters, leading to charge transfer and resonance effects. Relevant properties: (A) NPA charge of the Ag12 inner shells; (B) Electron affinity of Pd/Ag/Pt/Au; (C) $Ag_{\text{inner shell}}-S_{\text{terminal}}$ bond lengths average; (D) Resonance factor $|1/[(E_2-E_0-2\omega)(E_1-E_0-2\omega)]|$. E_1 , E_2 represent the energy of 2 absorption bands of $M_1Ag_{24}(SR)_{18}$ nanoclusters, and E_0 represents the energy of excitation light. Charge factors are obtained from previous report.³

Table S2: Calculated frequency-dependent hyperpolarizabilities obtained from the TD-DFT approach for $\text{Ag}_{25}(\text{SR})_{18}$ and doped $\text{M}_1\text{Ag}_{24}(\text{SR})_{18}$ nanoclusters at different wavelengths (with simplified SCH_3 and fully explicit DMBT ligands). Results for $\text{Ag}_{25}(\text{SR})_{18}$ and doped $\text{M}_1\text{Ag}_{24}(\text{SR})_{18}$ nanoclusters with full ligands in DCM solvent (CH_2Cl_2 – Dichloromethane) are highlighted (blue). Components are expressed in the molecular frame, using the formula given by “Clays and Persoons Hyper-Rayleigh scattering. Opportunities for molecular, Wavelength (nm) supramolecular, and device characterization by incoherent 2nd-order nonlinear light scattering: Academic Press”, 2001, are transformed in $\beta(2\omega)$ value which is therefore in the laboratory frame.

	550 nm	600 nm	650 nm	700 nm	750 nm	800 nm	850 nm	900 nm
$\text{Ag}_{25}(\text{SCH}_3)_{18}$	16	5809	26	10	7	5	4	3
$\text{Ag}_{25}\text{DMBT}_{18}$	27	874	703	42	25	19	17	15
$\text{Ag}_{25}\text{DMBT}_{18}$	50	718	3810	79	53	34	29	54
$\text{AuAg}_{24}(\text{SCH}_3)_{18}$	35000	20	8	5	4	3	3	2
$\text{AuAg}_{24}\text{DMBT}_{18}$	130	2600	35	20	15	13	12	11
$\text{AuAg}_{24}\text{DMBT}_{18}$	200	23486	76	42	32	27	24	23
$\text{PtAg}_{24}(\text{SCH}_3)_{18}$	2236	17	7	4	3	2	2	2
$\text{PtAg}_{24}\text{DMBT}_{18}$	253	532	47	26	20	16	14	13
$\text{PtAg}_{24}\text{DMBT}_{18}$	340	36376	106	49	35	27	25	23
$\text{PdAg}_{24}(\text{SCH}_3)_{18}$	15	1400	16	6	4	3	3	2
$\text{PdAg}_{24}\text{DMBT}_{18}$	34	92	5400	70	34	25	20	18
$\text{PdAg}_{24}\text{DMBT}_{18}$	42	127	28326	183	79	55	45	39

TDDFT calculations in DCM

* 10^{-30} esu

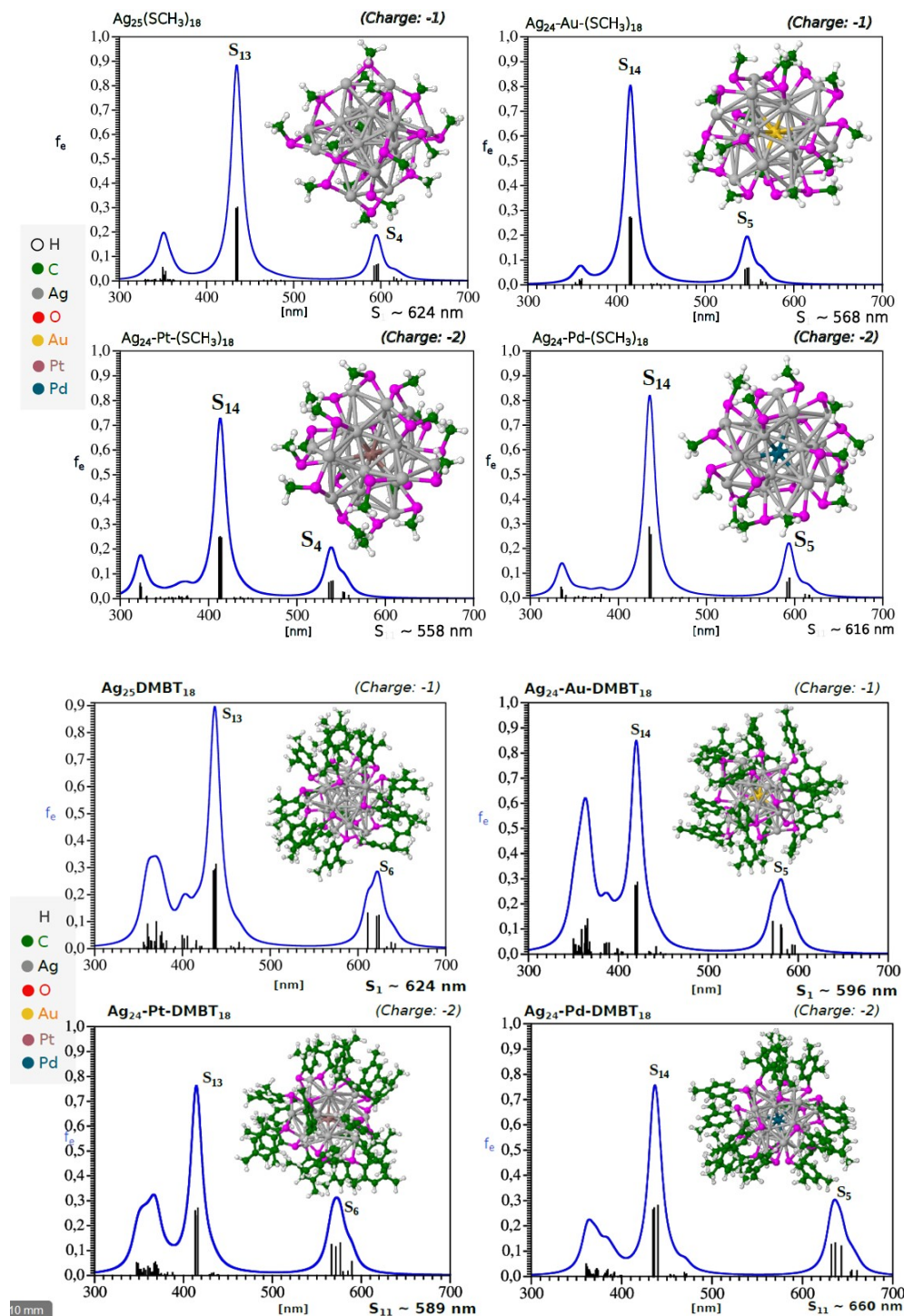


Figure S7. TD-DFT linear absorption spectrum for $\text{Ag}_{25}(\text{SR})_{18}$ and doped $\text{M}_1\text{Ag}_{24}(\text{SR})_{18}$ nanoclusters at different wavelengths with simplified SCH_3 (upper panel) and fully explicit DMBT ligands (lower panel).

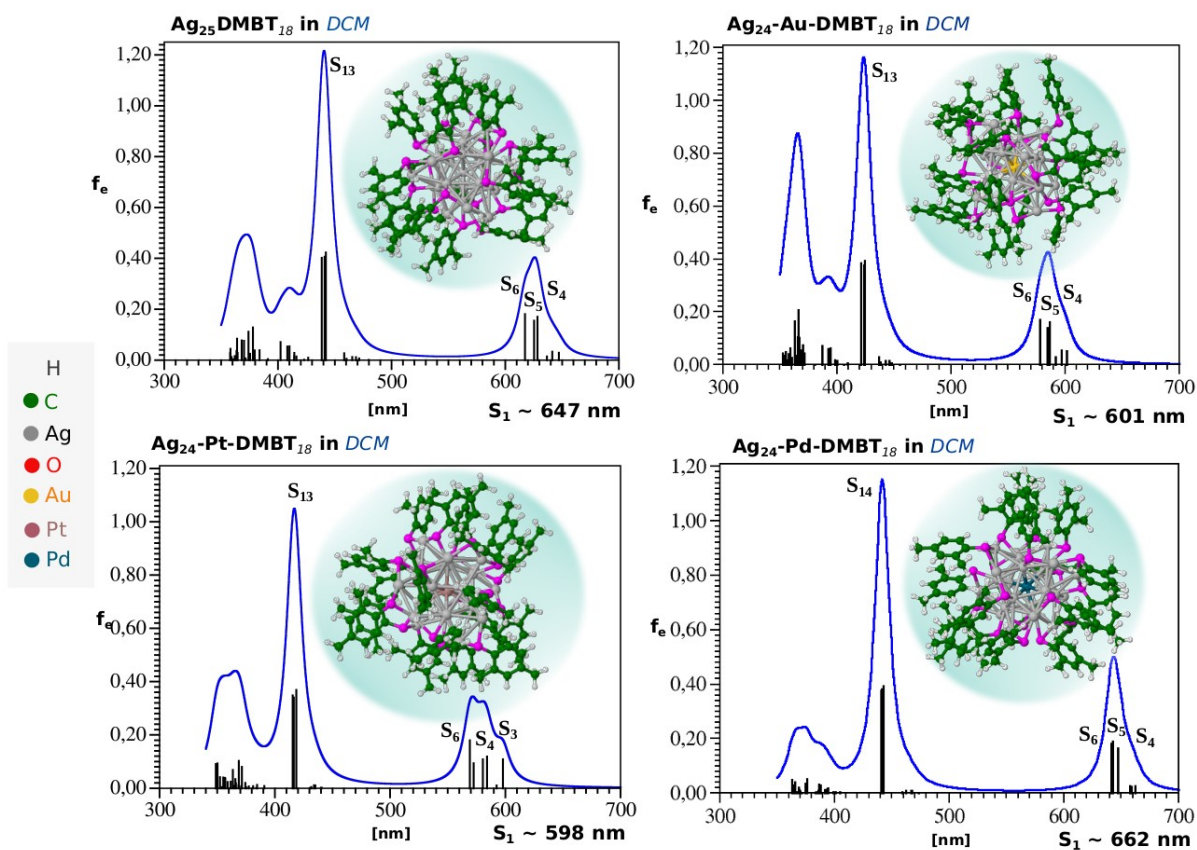


Figure S8. TD-DFT linear absorption spectrum for $\text{Ag}_{25}(\text{SR})_{18}$ and doped $\text{M}_1\text{Ag}_{24}(\text{SR})_{18}$ nanoclusters in DCM solvent (CH_2Cl_2 - Dichloromethane) at different wavelengths with fully explicit DMBT ligands.

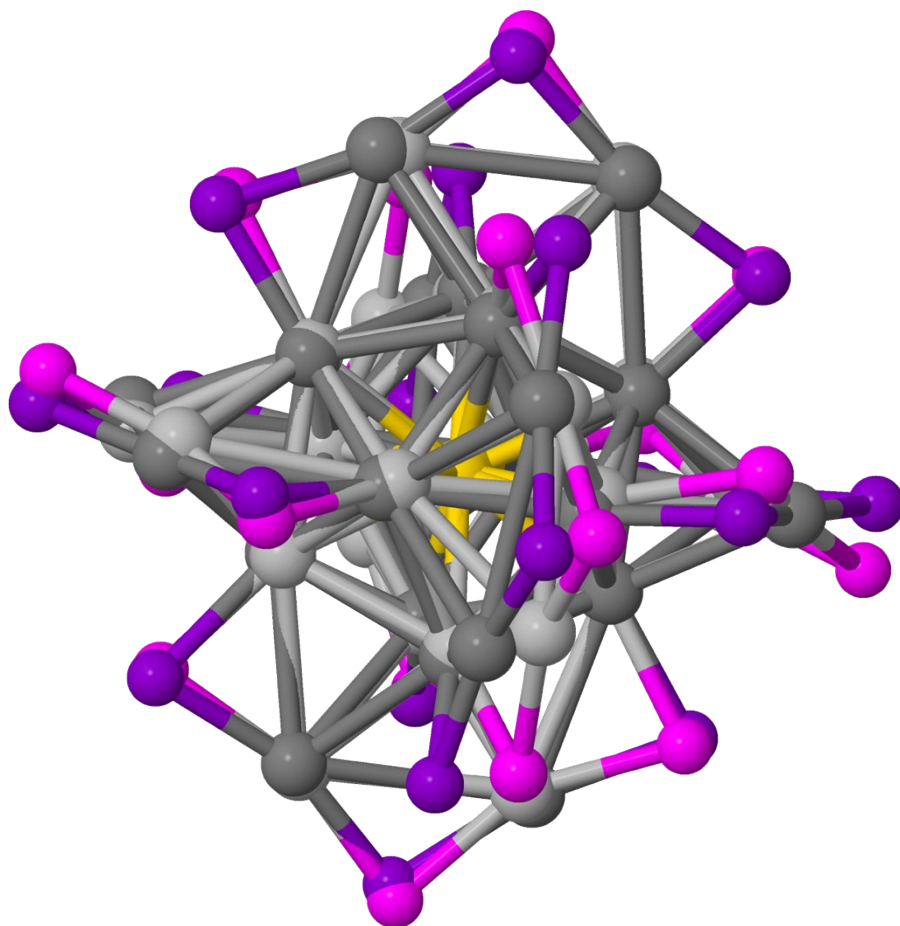


Figure S9: Representation of $\text{Au}_1\text{Ag}_{24}(\text{SR})_{18}$ metal core and staple motifs from different DFT geometries of the same nanocluster. $\text{Au}_1\text{Ag}_{24}(\text{SR})_{18}$ (I) is the DFT-optimized geometry from crystal structures in the present paper. $\text{Au}_1\text{Ag}_{24}(\text{SR})_{18}$ (II) is the DFT optimized geometry from Olesiak-Bańska et al.⁴ Dark grey for silver atoms and violet for sulfur atoms are chosen for geometry (I) and grey and magenta for geometry (II). Gold in the center is presented in yellow.

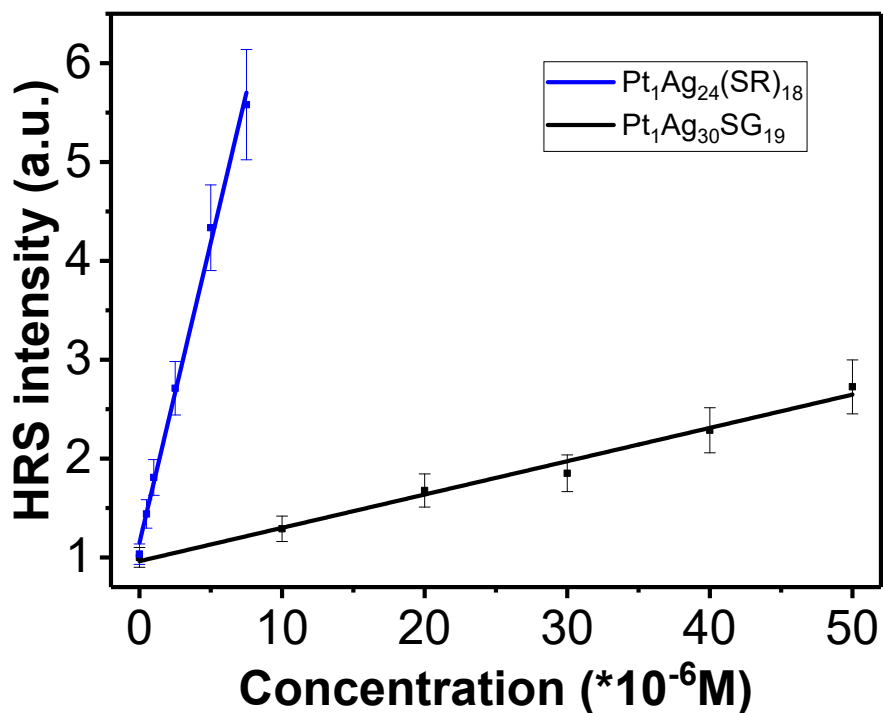


Figure S10: Plot of the HRS intensity for Pt-doped silver nanoclusters as a function of concentration. (with SR=DMBT and SG=glutathione)

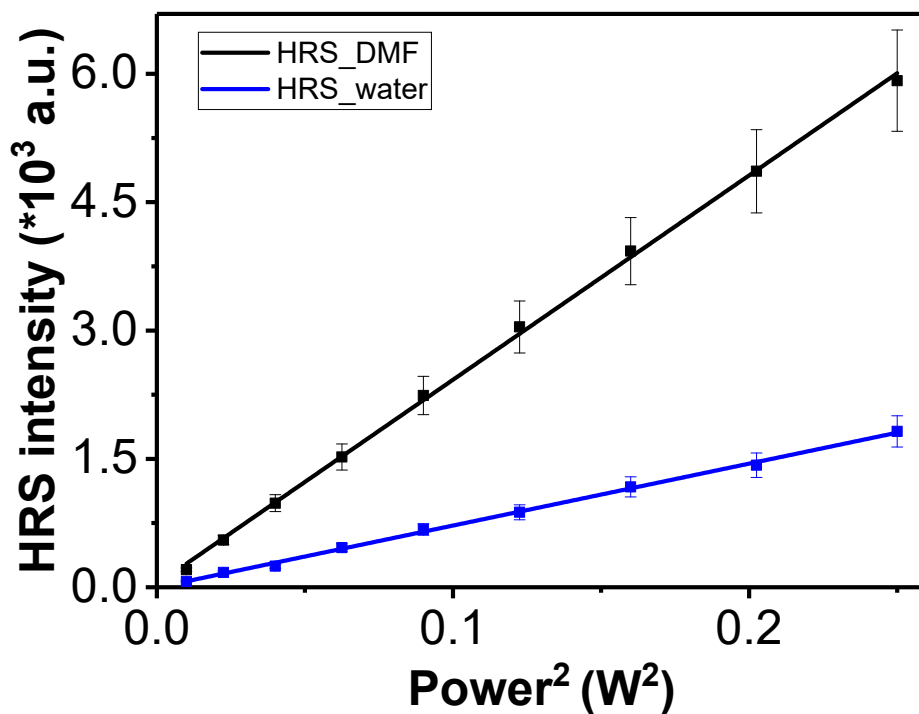


Figure S11: Plot of the HRS intensity for DMF and water as a function of $(\text{laser power})^2$ (at 800 nm laser excitation).

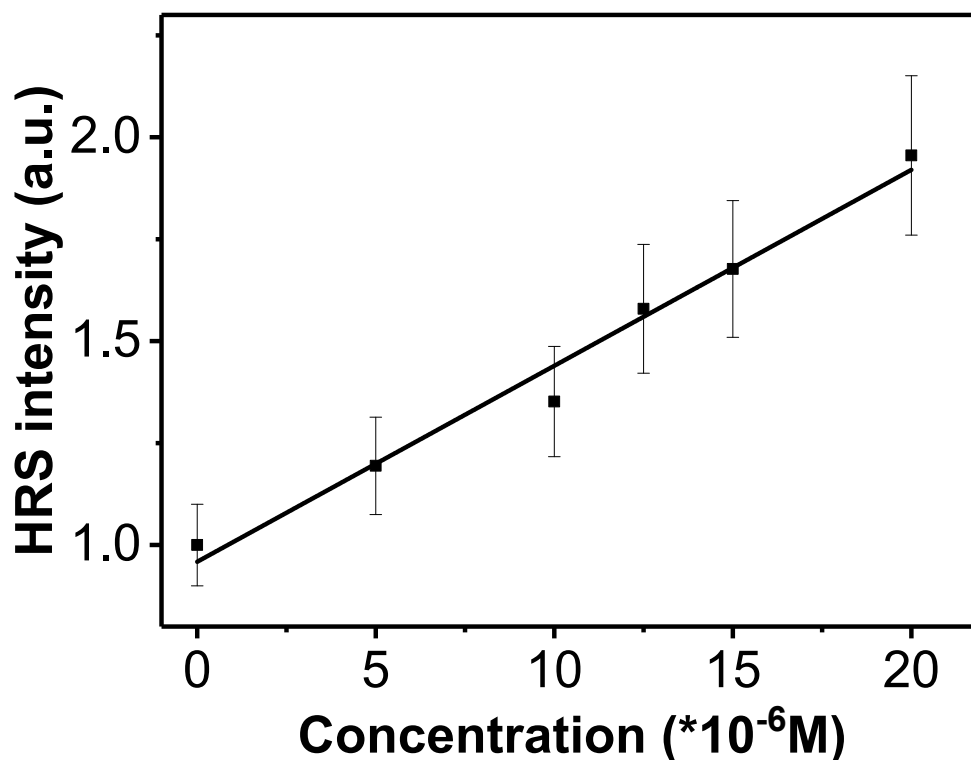


Figure S12: Plot of the HRS intensity for Au₂₅AcCys₁₈ nanoclusters as a function of concentration.

References

1. I. Russier-Antoine, F. Bertorelle, M. Vojkovic, D. Rayane, E. Salmon, C. Jonin, P. Dugourd, R. Antoine and P.-F. Brevet, *Nanoscale*, 2014, **6**, 13572-13578.
2. F. Bertorelle, I. Russier-Antoine, C. Comby-Zerbino, F. Chirot, P. Dugourd, P.-F. Brevet and R. Antoine, *ACS Omega*, 2018, **3**, 15635-15642.
3. X. Liu, J. Yuan, C. Yao, J. Chen, L. Li, X. Bao, J. Yang and Z. Wu, *The Journal of Physical Chemistry C*, 2017, **121**, 13848-13853.
4. A. Pniakowska, K. Kumaranchira Ramankutty, P. Obstarczyk, M. Perić Bakulić, Ž. Sanader Maršić, V. Bonačić-Koutecký, T. Bürgi and J. Olesiak-Bańska, *Angew. Chem. Int. Ed.*, 2022, **61**, e202209645.